Ice velocity determined using conventional and multiple-aperture InSAR

Citation for published version:
Gourmelen, N, Kim, SW, Shepherd, A, Park, JW, Sundal, AV, Björnsson, H & Pálsson, F 2011, 'Ice velocity determined using conventional and multiple-aperture InSAR', *Earth and Planetary Science Letters*, vol. 307, no. 1-2, pp. 156-160. https://doi.org/10.1016/j.epsl.2011.04.026

Digital Object Identifier (DOI):
10.1016/j.epsl.2011.04.026

Published In:
Earth and Planetary Science Letters

This is the author's final draft or 'post-print' version as submitted for publication. The final version was published in Earth and Planetary Science Letters copyright of Elsevier (2011).

Cite As: Gourmelen, N, Shepherd, A, Park, JW, Sundal, AV, Kim, SW, Björnsson, H & Pálsson, F 2011, 'Ice velocity determined using conventional and multiple-aperture InSAR' *Earth and Planetary Science Letters*, vol 307, no. 1-2, pp. 156-160.

DOI: 10.1016/j.epsl.2011.04.026

Ice velocity determined using conventional and multiple-aperture InSAR

N. Gourmelen[1], S. W. Kim[2], A. Shepherd[1], J.W. Park[1,3], A.V. Sundal[1], H. Björnsson[4], F. Pálsson[4]

[1] School of Earth and Environment, University of Leeds, Leeds, UK

[2] Department of Geoinformation Engineering, Sejong University, Seoul, South Korea.

[3] Earth System Sciences, Yonsei University, Seoul, South Korea

[4] Institute of Earth Sciences, University of Iceland, Reykjavík, Iceland

Abstract

We combine conventional Interferometric Synthetic Aperture Radar (InSAR) and Multiple Aperture InSAR (MAI) to determine the ice surface velocity on the Langjokull and Hofsjokull ice caps in Iceland in 1994. This approach allows the 20 principal ice cap outlets to be fully resolved. We show that MAI leads to displacement estimates of finer resolution (15 versus 150 m) and superior precision (5 versus 15 cm) to those afforded by the alternative technique of speckle tracking. Using SAR data acquired in ascending and descending orbits, we show that ice flows within 15° of the direction of maximum surface slope across 66 % of the ice caps. It is therefore possible to determine ice displacement over the majority of the ice caps using a single SAR image pair, thereby reducing errors associated with temporal fluctuations in ice flow.

Introduction

Repeat-pass Interferometric Synthetic Aperture Radar, or InSAR, is a remote sensing technique developed to recover ground motion from a pair of synthetic aperture radar (SAR) images acquired at two distinct time periods (Gabriel et al., 1989). The technique is a powerful tool because it requires virtually no field support, is an all-weather radar system, provides a high spatial density of measurements (up to one observation every 5 x 20 m^2), and typically offers instrumental precision to a few millimeters (Gabriel et al., 1989). InSAR has been successfully applied to measure ice displacement and to characterize fluctuations in the flow velocity of glaciers and ice sheets in response to climatic change (Gabriel et al., 1989; Joughin et al., 1996; Rignot and Kanagaratnam, 2006; Shepherd et al., 2001).

Current limitations of InSAR measurements over ice include: (1) a rapid degradation of phase coherence when the time interval separating the SAR images is larger than a few days, leading to measurement loss and uncertainty in areas of low coherence; and (2) insensitivity to surface displacement in the plane orthogonal to the vector of the radar Line-Of-Sight (LOS), resulting in the incapacity to detect motion in the direction of the satellite ground-track. The latter (geometric) limitation may be overcome by the use of SAR data acquired under multiple look angles (e.g. during ascending and descending orbits, with variable beam angles, or with adjacent tracks) (Wright et al., 2004; Gourmelen et al., 2007). This method, however, requires a specific region to have sufficient satellite coverage, to ensure that the measured displacement is constant during the interval between successive SAR data acquisition, conditions that are often violated. Alternatively, the features of SAR images may be tracked (also known as offset or speckle tracking) to recover along-track estimates of displacement (Gray et al., 2001). Tracking technique provides relatively coarse and sparse observations with regard to the optimum radar resolution, and performs poorly over ice when the temporal separation of SAR images is short (as is required for InSAR).

Multiple Aperture InSAR, or MAI, is a new technique applicable to SAR data from all available SAR instruments. MAI extends the sensitivity of InSAR to along-track displacement, thus allowing a complete recovery of the three-dimensional (3D) displacement field, using a single pair of SAR data and parallel flow assumption or two pairs of SAR images (Bechor and Zebker, 2006; Jung et al., 2009). It offers potentially enhanced precision over the technique of offset tracking over high coherence areas (Bechor and Zebker, 2006; Jung et al., 2009) and provides a capacity to sample across- and along-track displacements over the same time interval. MAI, like InSAR, is subject to rapid decorrelation over ice and is therefore limited to measurements made over a short time period, typically of a few days but this can vary depending on sensor characteristics and on ground conditions. We employ this novel technique, as well as conventional InSAR, to study the displacement field of the second and third largest ice caps in Iceland: Langjökull Ice Cap, or LIC, and Hofsjökull Ice Cap, or HIC (Figure 1).

Study Area

About 11 % (11,100 km^2) of Iceland is covered by temperate ice (Figure 1a), with an estimated total volume of 3,600 km^3. If all of this ice was to rapidly melt, global sea levels would rise by approximately 1 cm (Bjornsson and Palsson, 2008). The glaciers of Iceland are dynamically active and respond sensitively to climatic fluctuations (Bjornsson, 1979). During the little ice age glaciers extended, reaching a maximum extension around 1890. In the early 20th century, there was a general recession of Icelandic glaciers, the rate of which greatly accelerated in the 1930s and 1940s. The recession slowed after the 1960s but after 1995 increased to rates similar to that of the 1930s (Bjornsson, 1979). The techniques of InSAR and MAI allow us to monitor changes affecting the Icelandic glaciers from remote platforms (Palmer et al., 2009).

With an area of approximately 900 km^2 (in 2000) Langjökull is Iceland's second largest ice cap and has a mean surface elevation of 1080 m (Bjornsson and Palsson, 2008). Radio echo sounding has revealed a mean ice thickness of 210m and a maximum of 650m (Bjornsson and Palsson, 2008). The total ice volume of the LIC is estimated to be 190 km^3, which is equivalent to 0.5 mm of eustatic sea level rise (SLR). The southern outlet glaciers of Hagafellsjökull Vestri and Hagafellsjökull Eystri (Figure 1b) have experienced several surges over the last forty years, affecting ice velocity over an area of up to 200 km^2, the most recent being in 1999 (Bjornsson et al., 2003). The average annual net balance of the LIC, measured between 1996-97 and 2007-08, was equivalent to a loss of 1.3m of water. (m w eq.) (Bjornsson and Palsson, 2008).

Hofsjökull is Iceland's third largest ice cap and has an area of 890 km^2 (in 2000) and a mean surface elevation of 1245 m (Bjornsson and Palsson, 2008). While smaller in area than the LIC, the ice is thicker with a mean value of 225 m reaching a maximum of ~760 m, resulting in a greater ice volume of 200 km^3 (Bjornsson and Palsson, 2008). Several outlet glaciers reportedly surged around the time of our observations including Múlajökull, which surged in 1992 affecting an area of ~ 10 km^2 resulting in a terminus advance of several hundred metres (Bjornsson et al., 2003). The average annual net balance of the HIC measured between 1987-88 and 2005-06 was -0.53 m w.eq. (Bjornsson and Palsson, 2008; Sigurdsson et al., 2004; Sigurdsson et al., 2007).

Data and Methodology

We have processed a test set of SAR images from descending orbit, track 38, frame 2295, acquired on the 22 and 25 of February 1994 and from ascending orbit, track 30, frame 1305, acquired on the 24 and 27 of February 1994 by the European Remote Sensing 1 (ERS-1) satellite, during a 3-day repeat phase of acquisition. The descending and ascending SAR pairs have perpendicular baselines of 138 m and 306 m respectively. Using these data, we have produced two conventional interferograms and two MAI interferograms, as well as two speckle tracking offset maps for comparison purposes. Surface topography affects the conventional and MAI interferograms in different ways. To reduce topographic effects, we use a Digital Elevation Model (DEM, a 200m by 200m matrix grid) for LIC constructed from a Global Positioning System (GPS) profile survey (profiles about 1km apart) conducted in

April 1997 with a vertical accuracy between 2 and 5 meters, and a similar DEM for HIC based on precision barometric profile survey conducted in 1983 (Bjornsson, 1988).

The MAI interferograms were constructed following the method described by Jung et al. (2009), developed from the original MAI method proposed by Bechor and Zebker, (2006). MAI processing extracts the along-track component of surface deformation by first creating four sub-aperture Single-Look Complex (SLC) images from a pair of SAR scenes, forming one backward-looking and one forward-looking SLC from each SAR scene. Using the four SLCs, a backward-looking and a forward-looking interferogram are then produced from the interferometric combination of the two backward looking SLCs and of the two forward looking SLCs, respectively. In the final stage, the MAI interferogram is produced by a complex-conjugate multiplication of the forward-looking and backward-looking interferograms; the MAI phase is then equivalent to (Bechor and Zebker, 2006)

$$\phi_{MAI} = \phi_f - \phi_b, \tag{1}$$

where ϕ_{MAI}, ϕ_f, and ϕ_b, are the phase of the MAI-, forward-, and backward-looking interferograms, respectively. The MAI interferometric phase can be written as:

$$\phi_{MAI} = -\frac{4\pi}{l} n U_{MAI}, \tag{2}$$

where U_{MAI} is the surface displacement in the along-track direction, l is the effective antenna length, and n is the normalized squint angle. Here, l = 10 m and n = 0.5, a single fringe within an ERS-1 multiple aperture interferogram corresponds to 10 m of surface displacement in the along-track direction.

The MAI strategy reduces a number of error sources that are common to conventional InSAR. The symmetry between the forward- and backward-looking geometry, means that the range component and the sampled troposphere in the forward and backward looking interferograms are almost identical; consequently, the topographic and tropospheric contributions to the interferometric phase cancel out during the formation of the MAI interferogram (Bechor and Zebker, 2006). Also, the lower sensitivity of MAI to ground motion relative to conventional InSAR, reduces the occurrence of unwrapping errors due to high fringe rate. When compared to the results of conventional radar offset tracking over land, MAI offers a statistical improvement in the quality of along-track displacement measurements (Bechor and Zebker, 2006; Jung et al., 2009); if this is also true over ice, it would offer improved density of data over ice surfaces which are typically feature-poor (e.g. (Strozzi et al., 2002)). The InSAR processing is performed using the JPL/CALTECH software ROI_PAC, Rosen et al. (Rosen et al., 2004). The speckle tracking processing was performed using the method described by Strozzi et al., (2002). Speckle tracking results are dependent on the filtering and spatial averaging applied during processing. For the purpose of comparing speckle tracking with MAI , we use similar SLCs in both techniques, then perform the comparison by applying various spatial averaging during speckle tracking processing (Figure 2a). Ice motion was also computed at 23 locations over the LIC between April and October 2001 using differential GPS. The velocities were computed with regard to the REYK continuous GPS station in Reykjavík, and the station ISAKOT in south central Iceland (Palmer et al., 2009).

Results

The conventional (i.e. range component of the velocity) (Figure 1a), and the MAI (i.e. azimuth component of the velocity) (Figure 1b) interferograms show high coherence over both the LIC and HIC. Results over glaciers from both ice caps have a coherence of 0.7 or higher, which allows retrieval of the surface displacement field over the entire LIC and HIC area. We processed the MAI interferogram with and without accounting for the phase signal related to topography and, despite the sizeable altitude of ambiguity (~70 m for the descending pair and 30 m for the ascending pair), we observe no significant difference in the resulting interferogram; this confirms that MAI is insensitive to topography errors.

Given the altitude of ambiguity and expected DEM precision over Iceland we do not expect DEM related errors in our InSAR measurement to exceed 1 cm of equivalent displacement in the 3-day measurement period. MAI is insensitive to variation of the water vapor content in the troposphere (Bechor and Zebker, 2006). We tested our InSAR results for phase contribution due to variation of stratified water vapor content in the troposphere; no correlation was found between terrain height and phase in regions of no surface deformation and of significant altitude contrast (Elliott et al., 2008). We conclude that stratified water vapor plays a negligible role in our InSAR results. Furthermore, the standard deviation computed from the displacement field was only a few millimeters in those regions of no surface deformation, suggesting that turbulence within the troposphere plays a negligible role in our InSAR results. This is expected over ice given the low partial pressure of water vapor over ice.

We compute the displacement field, U_{DISP}, of both the LIC and the HIC in two ways. In the first approach, we use the LOS and MAI components of single SAR image pairs and assume that ice flows parallel to the local surface, we do this for independently for both ascending and descending orbits. In the second approach we combine the LOS and MAI observations recorded in descending and ascending orbits to produce deformation measurement from four look angles and compute the full 3D velocity field. In the first approach, we smooth the ice topography using a Gaussian filter with a radius equal to ten ice thickness (Bjornsson and Palsson, 2008) and compute the surface slopes in the azimuth (α_a) and range (α_r) directions (α_a and α_r are positive if the ground surface slopes toward the satellite and negative if the ground surface slopes away from the satellite). For each pixel, we determine U_{DISP} by solving the following equation:

$$U_{DISP} = \sqrt{\left(\frac{U_{MAI}}{\cos\alpha_a}\right)^2 + \left(\frac{U_{LOS}}{\sin(\alpha_r + \theta_i)}\right)^2} \qquad (3)$$

where θ_i is the radar incidence angle. The magnitude of U_{DISP} is shown in Figure 1c. Equation (3) is valid if the ice flow is not orthogonal to the plane formed by the slant range (LOS) and azimuth (MAI) directions, if $|\alpha_a| \neq 90^o$, and if $\alpha_r + \theta_i \neq [0^o, 180^o]$, which would significantly increase the error. Not one of these three situations occurs in our dataset. In the second approach, we combine the ascending and descending LOS and MAI measurements, which provide 4 independent look angles, to retrieve the full 3D displacement (Wright et al., 2004), with the assumption that the ice flow remains constant during the 5-day interval separating the ascending and descending observations.

Analysis and Discussion

We have compared the precision of the MAI technique with that of the speckle tracking technique, investigating both the relative measurement precision and the measurement resolution. We computed the standard deviation of the respective along track displacement map in an ice-free location which presents no evidence for surface deformation from analysis of our InSAR, MAI and speckle tracking results (see Figure 1a). Our analysis shows that MAI performs better than speckle tracking for typical levels of spatial averaging, the improvement provided by the MAI approach is considerable (up to a factor 11) when considering high-resolution datasets (Figure 2a). This allows to increases the density of measurement over a glacier, in particular in regions of low velocity (Figure 3).

Conventional InSAR processing (Figure 1a) detects the displacement (U_{LOS}) of nine outlet glaciers of the LIC, and of four of the HIC. With the aid of MAI processing (Figure 1b), we are able to detect the displacement (U_{MAI}) of the remaining three LIC glaciers, and of four remaining HIC glaciers (altogether a third of the total number of glaciers in both ice caps). The flow direction of these seven outlets is close to the satellite along track direction, which explains why their presence was undetected in a previous conventional InSAR study (Palmer et al., 2009). MAI measures displacement Þrístapajökull, Hagafellsjökull Vestari and Hagafellsjökull Eystri LIC outlets, and at Sátujökull, Illviðrajökull, Blautukvíslarjökull and Múlajökull outlets of HIC (Figure 1b,c).

Combining results from conventional InSAR and MAI in descending and ascending orbits, allows us to compute the first 3D horizontal velocity maps of the LIC and the HIC (Figure 1c). The complete velocity field of the LIC and of the HIC, obtained from the combination of both techniques, reveals a total of twelve (LIC) and eight (HIC) outlets in motion. The maximum velocity of the LIC outlets is 75 m yr^{-1}. The maximum velocity of the HIC is considerably faster, at 130 m yr^{-1}. A comparison between the velocity gradient and the surface gradient shows that 66% of the glacier area flows within 15 degrees of the surface gradient. The distribution of the displacement difference between the parallel flow solution and the full 3D solution shows that most of the difference is within the measurement precision range (Figure 2b).

The motion of Icelandic glaciers is highly variable with both seasonal and surge type acceleration (Bjornsson et al., 2003). We compared our 1994 velocity data to sparse observations of average summer glacier motion determined at the LIC during a GPS survey in the year 2001 to investigate the stability of ice flow over the intervening period. The root mean square (rms) difference between InSAR-MAI and GPS-determined velocity magnitudes is 17 m yr^{-1} (Figure 1d), revealing velocity discrepancies between the two datasets. Velocities measured by GPS from the 2001 survey are not systematically higher than those in 1994 determined by InSAR. Summer-average velocities measured by GPS are not systematically higher than the spring velocities determined by InSAR. Closer inspection reveals that the greatest discrepancies are restricted to certain outlets, and that the signs of these discrepancies tend to vary from one glacier to another. For example, the InSAR-MAI derived velocity rates are 20 cm higher for all 3 GPS rates for the outlet Geitlandsjökull, and 20 cm lower for all 4 GPS rates for the outlet Hagafellsjökull Vestri (Figure 1d), a significant departure with regard to the measurement error estimates. Potential explanations for such behaviour include seasonal fluctuations in flow, such as those observed at mountain and ice sheet outlet glaciers [e.g. (Zwally et al., 2002; Joughin et al., 2008)], and episodic fluctuations associated with glacier surges [e.g. (Fowler and Shiavi, 1998)]. Moreover, surging is typical of Icelandic glaciers, and has been documented at the south LIC outlets of Hagafellsjökull Vestri and Hagafellsjökull Eystri (Bjornsson et al., 2003), so we have interpreted the fluctuations to indicate similar behaviour.

Conclusions

We combine across-track (slant range) displacement measurements obtained from conventional InSAR and along-track (azimuth) displacement measurements obtained from MAI to produce the first 3D ice velocity map derived from an interferometric combination of a pair of ascending and a pair of descending SAR data. The approach enhances the precision of ice flow measurement by a factor of 2 for standard ground resolution (i.e. ~100 meters)

measurements and up to a factor of 10 for high ground resolution (i.e. ~10 meters) measurement as compared to a velocity solution based on InSAR and speckle tracking. The method allows us to resolve the flow of: 20 glaciers of the Langjökull and Hofsjökull ice caps in Iceland in spring 1994; 13 from InSAR and 7 from MAI, due to the direction of flow versus the radar axes. Average ice velocity over the 3-day time interval reaches a maximum of 75 m yr^{-1} and 130 m yr^{-1} at the LIC and HIC, respectively. We show further that ice flows within 15 degrees of the slope gradient for 66% of the HIC and LIC. Our method provides a new and improved capacity to detect fluctuations and permanent changes in ice flow from spaceborne platforms.

Acknowledgements

This work was supported by the UK Natural Environment Research Council Antarctic Funding Initiative (NE/E014089/1) and by a Philip Leverhulme Prize to A.S.

Figures

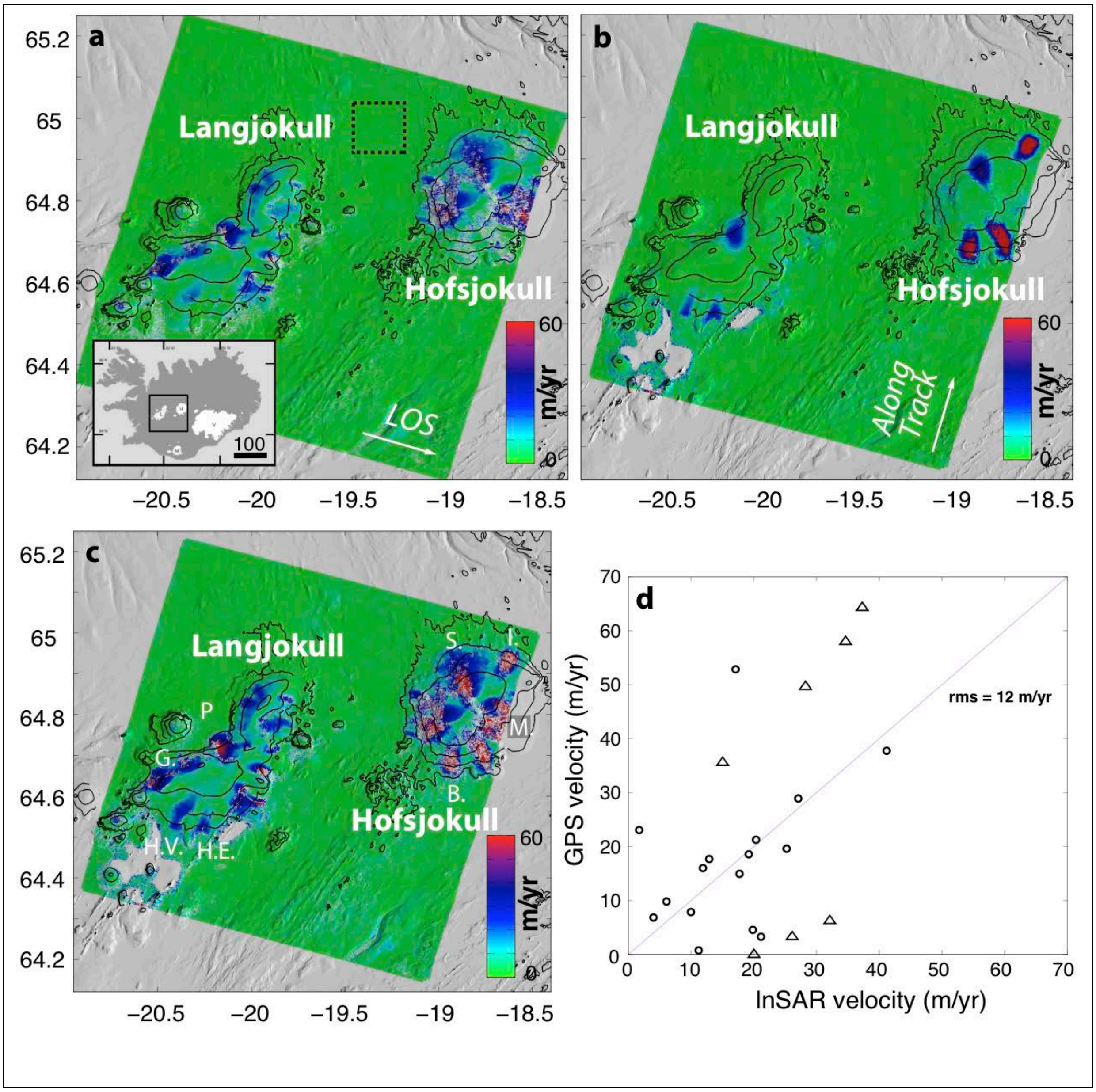

Figure 1: Motion of the Langjökull and Hofsjökull ice caps and topographic contours (colour) superimposed over the terrain in shaded relief (grey). a - Conventional InSAR across-track component of the velocity vector with a map of Iceland showing the study location (inset) and the location chosen for computation of the displacement standard deviation (dashed area); b - MAI along-track component of the velocity vector; c - Velocity magnitude determined from combining a and b and assuming surface parallel ice flow. Glaciers

identified are Hagafellsjökull Vestari, H.V., Hagafellsjökull Eystri, H.E., Þrístapajökull, P., Sátujökull, S., Illviðrajökull I., Blautukvíslarjökull, B., Múlajökull M., and Geitlandsjökull, G. glaciers; d - Difference between InSAR-MAI and GPS determined velocities as a function of the ice flow direction. The measurement vector heading for conventional (LOS), and MAI (MAI) measurement is indicated for comparison. Measurements at Geitlandsjokull and Hagafellsjökull Vestri (triangles) show greater variance than those recorded elsewhere (circles). RMS is computed using the GPS measurements indicated by the circle symbols.

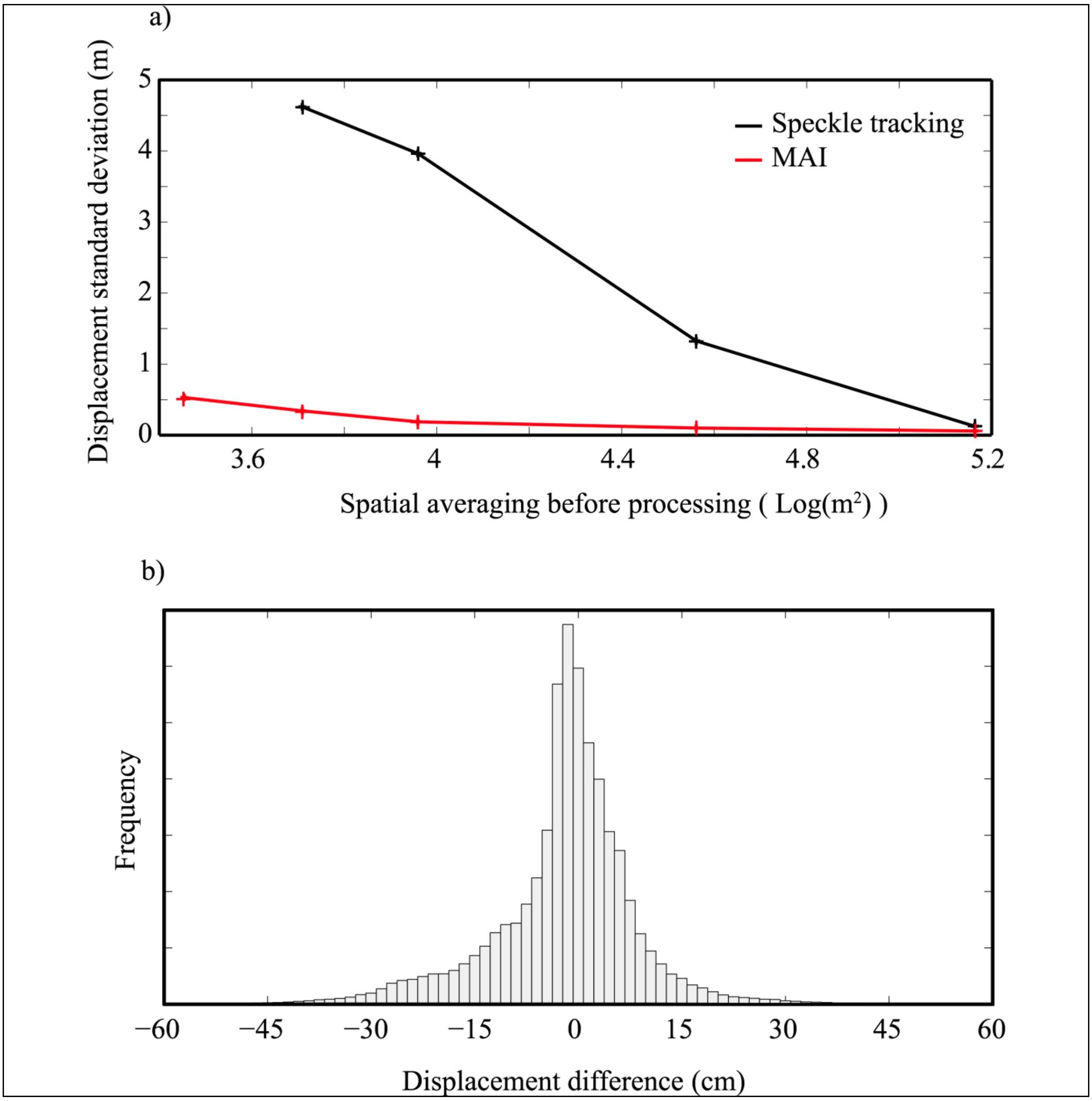

Figure 2: a. Standard deviation of displacement computed using MAI and speckle tracking versus measurement resolution in a region of no motion. MAI outperforms speckle tracking at all resolutions and by up to a factor of 11 for the highest common resolution (20 by 20 m). b. Histogram of the difference between displacement above 5cm estimated assuming surface parallel flow (ascending and descending solutions combined) and the full 3D-solution.

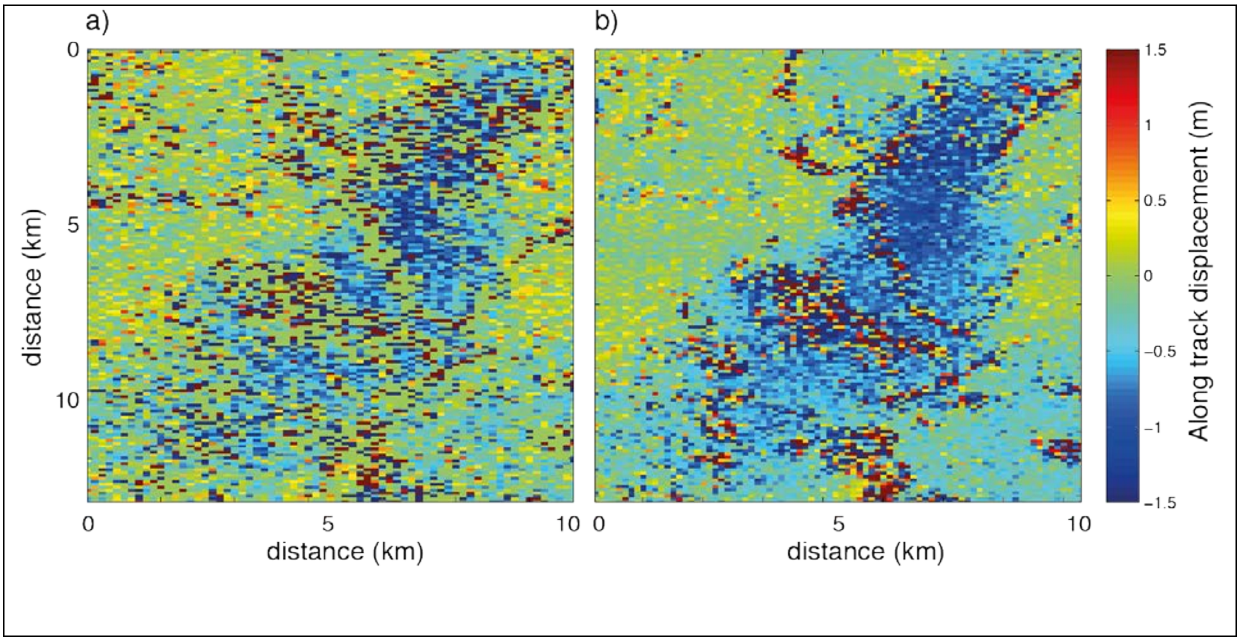

Figure 3: Ice displacement computed by a) Speckle tracking and b) MAI over the Illviðrajökull glacier, HIC, using no filtering and identical ground pixel resolution. MAI shows better resolution of the glacier velocity in particular in region of slow motion.

References

Bechor, N. B. D. and Zebker, H. A., 2006. Measuring two-dimensional movements using a single InSAR pair. Geophysical Research Letters. 33.

Bjornsson, H., 1979. Glaciers in Iceland. Jokull. 29, 74-80.

Bjornsson, H., 1988. Hydrology of ice caps in volcanic regions. 1-139.

Bjornsson, H., Palsson, F., Sigurdsson, O., Flowers, G.E., 2003. Surges of glaciers in Iceland.

Bjornsson, H. and Palsson, F., 2008. Icelandic glaciers. Jokull. 58, 365-386.

Elliott, J. R., Biggs, J., Parsons, B., Wright, T. J., 2008. InSAR slip rate determination on the Altyn Tagh Fault, northern Tibet, in the presence of topographically correlated atmospheric delays. Geophysical Research Letters. 35, L12309.

Fowler, A. C. and Shiavi, E., 1998. A theory of ice-sheet surges. Journal of Glaciology. 44, 104-118.

Gabriel, A. K., Goldstein, R. M., Zebker, H. A., 1989. Mapping Small Elevation Changes Over Large Areas - Differential Radar Interferometry. Journal of Geophysical Research-Solid Earth and Planets. 94, 9183-9191.

Gourmelen, N., Amelung, F., Casu, F., Manzo, M., Lanari, R., 2007. Mining-related ground deformation in Crescent Valley, Nevada: Implications for sparse GPS networks. Geophysical Research Letters. 34, L09309.

Gray, A. L., Short, N., Mattar, K. E., Jezek, K. C., 2001. Velocities and flux of the Filchner ice shelf and its tributaries determined from speckle tracking interferometry. Canadian Journal of Remote Sensing. 27, 193-206.

Joughin, I., Das, S. B., King, M. A., Smith, B. E., Howat, I. M., Moon, T., 2008. Seasonal speedup along the western flank of the Greenland Ice Sheet. Science. 320, 781-783.

Joughin, I., Kwok, R., Fahnestock, M., 1996. Estimation of ice-sheet motion using satellite radar interferometry: Method and error analysis with application to Humboldt Glacier, Greenland. Journal of Glaciology. 42, 564-575.

Jung, H., Won, J., Kim, S., 2009. An Improvement of the Performance of Multiple Aperture SAR Interferometry (MAI). IEEE Transactions on Geoscience and Remote Sensing.

Palmer, S., Shepherd, A., Bjornsson, H., Palsson, F., 2009. Ice velocity measurements of Langjökull, Iceland, from interferometric synthetic aperture radar. Journal of Glaciology. 55, 834-838.

Rignot, E. and Kanagaratnam, P., 2006. Changes in the velocity structure of the Greenland ice sheet. Science. 311, 986-990.

Rosen, P. A., Henley, S., Peltzer, G., Simons, M., 2004. Updated Repeat Orbit Interferometry Package Released. Eos Transaction American Geophysical Union. 85.

Shepherd, A., Wingham, D. J., Mansley, J. A. D., Corr, H. F. J., 2001. Inland thinning of Pine Island Glacier, West Antarctica. Science. 291, 862-864.

Sigurdsson, O., Thorsteinsson, T., Ágústsson, S. M., Einarsson, B., 2004. Afkoma Hofsjökuls 1997-2004. (Mass balanceof Hofsjökull 1997-2004). OS-2004/029, .

Sigurdsson, O., Jonsson, T., Johannesson, T., 2007. Relation between glacier-termini variations and summer temperature in Iceland since 1930. Annals of Glaciology, Vol 46, 2007. 46, 170-176.

Strozzi, T., Luckman, A., Murray, T., Wegmuller, U., Werner, C. L., 2002. Glacier motion estimation using SAR offset-tracking procedures. IEEE Transactions on Geoscience and Remote Sensing. 40, 2384-2391.

Wright, T. J., Parsons, B. E., Lu, Z., 2004. Toward mapping surface deformation in three dimensions using InSAR. Geophysical Research Letters. 31, L01607.

Zwally, H. J., Abdalati, W., Herring, T., Larson, K., Saba, J., Steffen, K., 2002. Surface melt-induced acceleration of Greenland ice-sheet flow. Science. 297, 218-222.